Organic Process Research & Development **2003**, *7*, 1007−1016

Combined Effect of Polymorphism and Process on Preferential Crystallization: Example with (±)-5(4′-Methylphenyl)-5-methylhydantoin

L. Courvoisier, L. Mignot, M. N. Petit, and G. Coquerel*

Unité de Croissance Cristalline et de Modélisation Molećulaire (UC²M²), SMS UPRES EA 2659, IRCOF, Université de Rouen, Rue Lucien Tesnière, F-76 821 Mont Saint Aignan Cedex, France

Abstract:

The structural data of two varieties of the title compound as well as the corresponding irreversible polymorphic transition are detailed. Although extensive structural analogies are pointed out, the transition is of destructive/reconstructive type with a poor rate requiring days or even weeks for completion. Without seeding, evidence of epitaxial nucleation is given. The genuine impact of polymorphism on the preferential crystallization is highlighted. The greater the departure from thermodynamic equilibrium the greater the differences between the courses of the entrainments initiated with a given polymorph. The best result in terms of robustness, yield, and conditions for up-scaling is obtained by using a combination of (i) a smooth crystallization process (auto-seeded and polythermic: AS3PC), (ii) the use of the stable polymorph, (iii) a pretreatment of the solid particles designed to enlarge the surface of the solid phase ready for the crystal growth as soon as the cooling program is launched.

Introduction

According to the current knowledge, only 5−10% of all chiral organic components crystallize as conglomerates (i.e. the racemic mixture is composed of an equal mixture of crystals which contain only one enantiomer) and 90−95% as racemic compounds or solid solution (minor proportion). As the separation of enantiomers via diastereomeric salt can be an expensive and time-consuming process that is also occasionally accompanied by technical problems (filterability, recycling of the resolving agents, etc.), the separation of enantiomers by preferential crystallization (PC hereafter, also called resolution by entrainment) is an attractive alternative which, however, is only applicable to conglomerates. This method is based on the selective crystallization of a single enantiomer, for a certain period of time, out of a supersaturated close-to-racemic solution. When the driving force (supersaturation) is created by cooling only, two processes can be applied: the classic[1] Seeded isothermal preferential crystallization (SIPC) and a variant developed in our laboratory,[2,3] the auto-seeded programmed polythermic preferential crystallization (AS3PC).

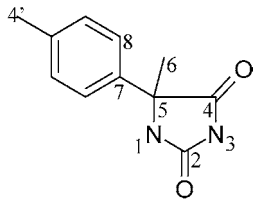

Figure 1. **Developed formula of the (±)17H.**

Table 1. **Specific rotatory power of 17H solutions vs wavelength (1 g/100 mL, ethanol)**

λ (nm)	578	546	436	365
$[\alpha_0]_{20}$ (deg)	110	127	234	418

In continuity with efforts designed to investigate the phenomena in competition during the stereoselective crystallization,[4−6] this contribution aims at determining the joint incidence of polymorphism and crystallization process on the course and the performance of the PC. In a first step, the crystallographic structure of the 17H polymorphs will be presented. Then, physicochemical properties (solubility, polymorphic transition) of the title compound will be detailed, and the mechanism of the polymorphic transition in relation with the structural analogies will be discussed. In a second step, the impact of polymorphism on SIPC and AS3PC will be examined.

Overview of the Monoclinic and Orthorhombic Forms of the 5(4′-Methyl phenyl)-5-methylhydantoin

The 5(4′-methylphenyl)-5-methylhydantoin is a chiral molecule (17H hereafter; Figure 1, Table 1) which crystallizes as a conglomerate and exhibits polymorphism. Synthesis of 17H is carried out using the one-pot Bücherer's reaction from the corresponding ketone (4′-methylacetophenone).[7] The enantiomers can be resolved by semipreparative HPLC Chirobiotic T column, 250 mm × 10 mm × 10 μm (ASTEC Inc.), mobile phase: methanol 1 mL/min, UV detector: λ = 225 nm or by using diastereomeric salts with α-methylbenzylamine.[8]

Two polymorphic forms have been experimentally identified for the enantiomers of 17H: an orthorhombic form

* Corresponding author. Fax +33 (0) 2 35 14 71 38. E-mail: Gerard.Coquerel@univ-rouen.fr.

(1) Jacques, J.; Collet, A.; Wilen S. H. *Enantiomers, Racemates and Resolution*; Krieger Publishing Company: Malabar, Florida, 1994.
(2) Courvoisier, L.; Ndzie, E.; Petit, M. N.; Sprendgard, U.; Coquerel, G. *Chem. Lett.* **2001**, *4*, 364.
(3) Coquerel, G.; Petit, M. N.; Bouaziz, R. EP 0720.595 B1/1995, *Chem. Abstr.* **1995**, *123*, 255843c.
(4) Courvoisier, L.; Gervais, C.; Mignot, L.; Petit, M. N.; Coquerel, G. *J. Phys. IV France* **2001**, *11*, 10−71.
(5) Houllemare-Druot, S.; Coquerel, G. *J. Chem. Soc., Perkin Trans. 2* **1998**, 2211.
(6) Dufour, F.; Gervais, C.; Petit, M. N.; Perez, G.; Coquerel, G. *J. Chem. Soc., Perkin Trans. 2* **2001**, *10*, 2022.
(7) Bücherer, H. T.; Lieb, V. A. *J. Prakt. Chem.* **1934**, *141*, 5.
(8) Coquerel, G.; Petit. M. N.; Bouaziz R.; Depernet D. *Chirality* **1992**, *4*, 400.

10.1021/op030022g CCC: $25.00 © 2003 American Chemical Society
Published on Web 11/21/2003

Table 2. **Crystallographic parameters of 17H polymorphs**

form	label	space group	Z	*a*(Å)	*b*(Å)	*c*(Å)	*β*(deg)	*V*(Å^3)
monoclinic	M	$P2_1$	2	11.732	6.253	7.362	103.79	525
orthorhombic	O	$P2_12_12_1$	4	22.757	6.256	7.344	90	1046

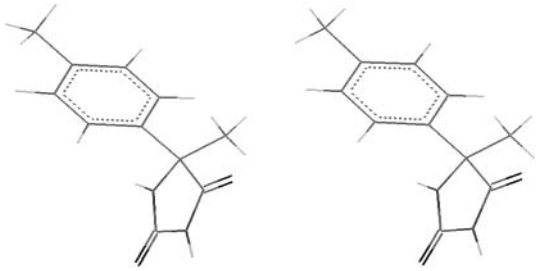

Figure 2. **Molecular conformation of 17H in the crystal structures: (left) monoclinic variety, (right) orthorhombic variety.**

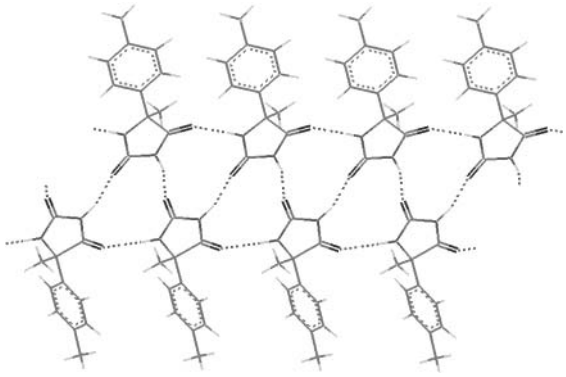

Figure 3. **Molecular ribbons parallel to the *b* axis observed in the two structures of 17H.**

($17H_O$ hereafter) which is the thermodynamically stable form under ambient conditions up to fusion and a less stable monoclinic form ($17H_M$ hereafter). No racemic compound has been identified thus far even when using harsh conditions of precipitation.[6] Therefore, two conglomerates exist for the racemic mixture (stable and unstable). The crystallographic parameters of the polymorphs are summarized in Tables 2, 3, and 4. The molecular conformations and crystal packing are illustrated by Figures 2, 3, 4, and 5. The two forms show extensive similarities, which result from (i) almost identical *b* and *c* crystallographic parameters (Table 2) and (ii) similar molecular conformations (Figure 2): the structures only differ by the rotation of the 4′-methyl group (Figure 1), (iii)

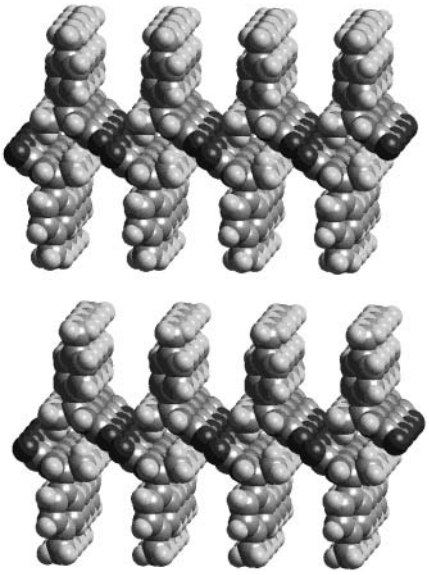

Figure 4. **Identical molecular slices (100) of the monoclinic form (top) and (200) of orthorhombic form (bottom) of 17H.**

identical hydrogen bond networks involving every heteroatom (Table 4, Figure 3), (iv) identical molecular ribbons parallel to the *b* axis (Figure 3) and involving every hydrogen bond, (v) identical molecular slices: (100) monoclinic form = (200) orthorhombic form (Figure 4).

Basic Principles of Preferential Crystallization

Two representations of the heterogeneous equilibria between two enantiomers (*R*, *S*) crystallizing as a stable conglomerate and a solvent A are useful in the description of the preferential crystallization considered in this study (Figure 6):

- ***the classical projection onto the isothermal section at T_{Fa} or T_{FA},***

- ***the isoplethal section*** which allows the visualization of the route followed by the solution point on cooling (as long as the same stoichiometric phase crystallizes, the solution point evolves in a plane parallel to *T* axis containing also the vertical axis corresponding to the crystallizing phase at different temperatures). In the case of interest here, on cooling, the crystallization of *R* can be monitored in the *R*−*Y* section corresponding to the relation: $X_A/X_S = (1 - Y)/Y =$ constant, where X_A and X_S stand respectively for the mass fraction of the solvent and of *S*.

Table 3. **Pertinent dihedral angles (deg) of 17H polymorphs (atom numbers, see Figure 1)**

form	$N_1-C_5-C_7-C_8$	$C_2-N_1-C_5-C_6$	$C_2-N_1-C_5-C_4$	$N_3-C_2-N_1-C_5$	$C_4-N_3-C_2-N_1$
monoclinic	−11.2	118.6	2.2	−0.8	−1.3
orthorhombic	−10.4	119.3	2.7	−1.2	−1.1

Table 4. **Hydrogen-bond lengths (Å) and angles (deg) in 17H polymorphs (atom numbers, see Figure 1)**

form	$d(O_{C4}\cdots N_1)$	$d(O_{C4}\cdots H_{N1})$	$d(O_{C2}\cdots N_3)$	$d(O_{C2}\cdots H_{N3})$	$(OC_4\cdots H_{N1})$	$(OC_2\cdots H_{N3})$
monoclinic	2.90	1.97	2.77	1.80	176.7	160.2
orthorhombic	2.88	1.87	2.78	1.82	179.3	161.4

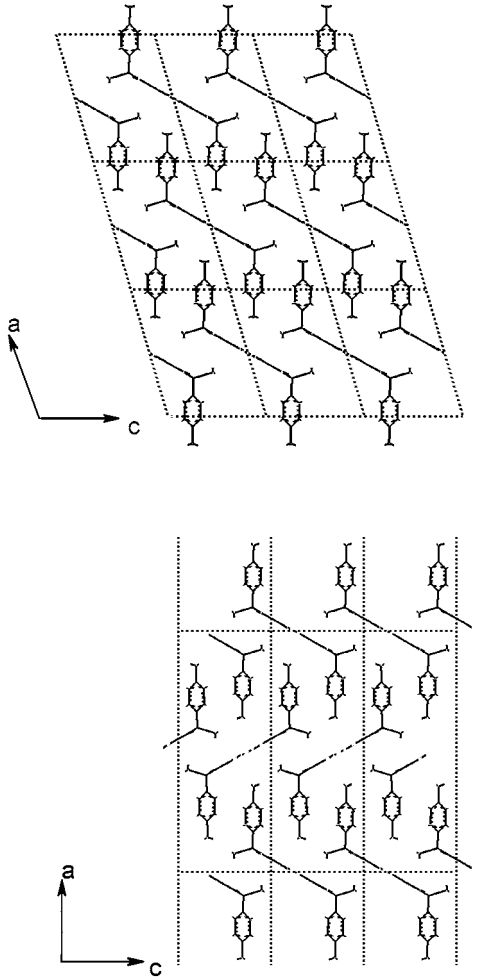

Figure 5. **Projection along b of the monoclinic polymorph (top) and orthorhombic polymorph (bottom) of 17H showing the difference of packing along the a direction.**

Seeded and Isothermal Preferential Crystallization Process (SIPC). The system (Figure 6, top) composed of solvent, racemic mixture (±), and an enantiomeric excess (e.g. *M* mass units of the *R* enantiomer) is homogenized at T_D (solution *E* (*E*, T_D)). A rapid cooling from T_D to T_{Fa}, creates the driving force (i.e., supersaturation) of the preferential crystallization without any nucleation. At T_{Fa}, the solution, continuously stirred, is seeded with pure crystals of the enantiomer that is initially in excess triggering a high nucleation rate. If we neglect the exothermic effect due to the crystallization, the solution point moves from (*E*; T_{Fa}) to (F_a; T_{Fa}) resulting from the isothermal stereoselective nucleation and crystal growth of the enantiomer *R*. Thus, at the end of this single run, the mother liquor contains an excess of the counter enantiomer *S* and 2*M* mass units of solid are isolated by filtration. Thus, 2*M* mass units of (±) are added to the mother liquor to yield a system with *M* mass of the counter enantiomer *S* and homogenized at T_D (solution *E*′). A fast cooling from T_D to T_{Fa} followed by seeding with pure crystals of *S* induces the PC of the enantiomer in excess. The process can be continued by repeating this cycle of operations and affords alternately *R* and *S* enantiomers.

Auto-Seeded and Polythermic Preferential Crystallization Process (AS3PC). The initial system (Figure 6, bottom), *E* mixture, containing an enantiomeric excess *M*′ of *R* is heated at T_B so that only the *S* enantiomer in default is completely dissolved . The suspension is then composed

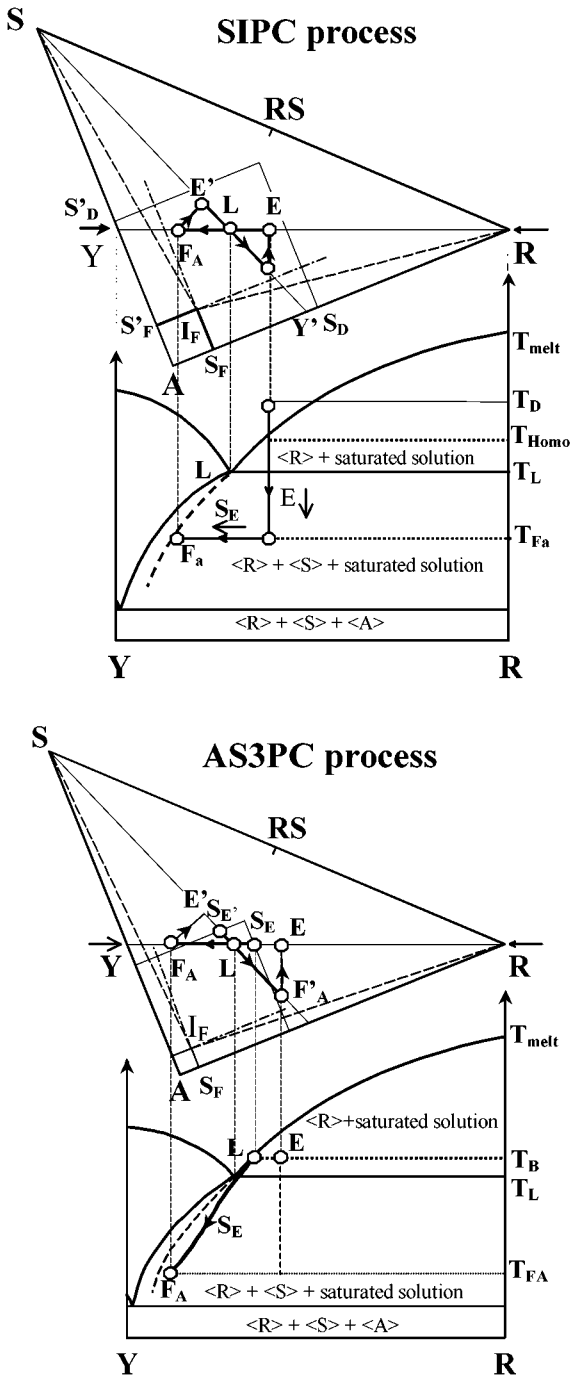

Figure 6. **Polythermic projections and isoplethal section of a ternary system describing SIPC and AS3PC processes (for more detailed explanations of the ternary phase diagram, see refs 3 and 5). *R* and *S* stand respectively for the pure enantiomer *R* and the pure enantiomer *S*. T_L: temperature of dissolution of the racemic mixture. $T_{Fa} = TF_{SIPC}$: filtration temperature for SIPC process. $T_{FA} = TF_{AS3PC}$: filtration temperature for AS3PC process. T_{Homo}: temperature of complete homogenization (racemic mixture plus enantiomeric excess). T_D: starting temperature for SIPC process $T_D > T_{Homo}$. T_B: starting temperature for AS3PC process ($T_{Homo} > T_B > T_L$). S_D, S_F: solubility of the enantiomer *R* at T_D and T_F respectively. S'_D, S'_F: solubility of the enantiomer *S* at T_D and T_F respectively.**

Table 5. **Solubilities (% w/w) in acetone**

temperature (K)	solubility of racemic mixture (S %w/w) (orthorhombic form)	solubility of pure enantiomer (S' %w/w) (monoclinic form)	solubility of pure enantiomer (S'' %w/w) (orthorhombic form)
298	8.89	2.87	2.85
312	10.23	3.36	3.34
318	11.62	3.85	3.83

Table 6. **Solubilities (% w/w) in 2-methoxyethanol**

temperature (K)	solubility of racemic mixture (S %w/w) (orthorhombic form)	solubility of pure enantiomer (S' %w/w) (monoclinic form)	solubility of pure enantiomer (S'' %w/w) (orthorhombic form)
287	12.9	6.79	6.78
298	14.4	7.52	7.49
312	17.0	8.93	8.91

of crystals of the enantiomer that is in excess and in thermodynamic equilibrium with its saturated solution S_E. In practice, this is carried out by an adjustment of the initial temperature at T_B (in first approximation: $T_B = (T_L + T_{homo})/2$). The points (E, T_B) and (S_E, T_B) do not coincide at the beginning of the process. The suspension is then submitted to a slow enough cooling program and stirring mode without any need of additional seeds; the system is self-seeded by crystals of the pure enantiomer which represent, according to the precise value of T_B, between 25 to almost 50% of the future crops. During the crystallization, S_E moves close to the metastable solubility curve of the enantiomer initially in excess with the following coordinates (S_E, T_X) where $T_L \geq T_X \geq T_{FA}$. At the end of the entrainment, (F_A, T_{FA}), the crystals of the R enantiomer are collected by filtration; $2M'$ mass units are isolated. The mother liquor contains an excess of the counter enantiomer S. $2M'$ mass units of (±) are then added to obtain the system (represented by E') constituted of S crystals in equilibrium with the saturated solution S'_E at T_B. From T_B to T_{FA} the same cooling program, stirring mode and stirring rate are applied; $2M'$ mass units of the enantiomer S are isolated. The process can be continued by repeating this cycle of operations and offers alternately $2M'$ mass units of R and S enantiomers.

Results. Discussion

Mechanism of the Polymorphic Transformation in Connection with the Structural Analogies. Kinetic of the Transition. The only difference between the two polymorphic forms concerns the packing of the (100) slices along the a direction (Figure 5). In the metastable monoclinic packing, there is a simple translation whereas in the stable orthorhombic packing, the binary screw axis 2_1 parallel to the a direction imposes an alternate orientation of the (200) orthorhombic slices ($(200)_O$ hereafter). These extensive structural analogies between the two polymorphic forms fall into the derived crystal packing[9] (DCP) model. This model allows the prediction of new lattices from a known crystal structure. The first operation of this two-step procedure consists of extracting a one- or two-dimensional periodic fragment (PF) from the mother structure. Subsequently, different sets of symmetry operators are added to generate new three-dimensional lattices. The slice (100) of the monoclinic form ($(100)_M$ hereafter) is of low energy and can be selected as periodic fragment. Then, a two-fold screw axis normal to PF and located at $y = 0$ is added to regenerate a 3D periodic lattice. After minimization (the daughter phases were minimized using the open force field module of the Cerius[2] software [force field: *Dreiding* 2.21[10] and Ewald summation for both van der Waals and Coulombic interactions, ESP charges derived from *Gaussian*94,[11] basic set B3LYP, method 6-G31**]), the difference in lattice energy ($E_O - E_M$) between the polymorphs is estimated to 0.3 kJ mol^{-1}. To reinforce the DCP model conclusions and to check that no other variety is present in the solid (including no unstable racemic compound for the racemic mixture), X-ray powder diffraction data (XRPD hereafter, diffractometer Siemens D5005) were established for the two polymorphic forms and compared to those calculated from the crystal structures using the Cerius[2] software.[12] Results (Figure 7) show that experimental data are quite similar to calculated values.

Results summarized in Tables 5 and 6 show that, whatever the solvent used and the temperature ranges explored, the solubilities of the two polymorphs are very close but always in favor of the orthorhombic form (the less soluble). Therefore, the monoclinic polymorph displays a monotropic behaviour in the range of temperature studied. In accordance with the Ostwald law of stages,[13] simple recrystallization in acetone (at 298 K) or in 2-methoxyethanol (at 287 K) always leads to the monoclinic form.

According to the structural features depicted above, the irreversible transformation $17H_M \rightarrow 17H_O$ cannot proceed via a continuous process but by means of a destructive/

(9) Gervais, C.; Coquerel, G. *Acta Crystallogr.* **2002**, *B 58*, 662.
(10) Mayo, S. L.; Olafson, B. D.; Goddard, W. A., III. *J. Phys. Chem.* **1990**, *94*, 8897.
(11) Frish, M. J.; Trucks, G. W.; Schlegel, H. P.; Gill, P. M. W.; Johnson, B. G.; Robb, M. A.; Cheseman, T. A. K.; Petersson, G. A.; Montgomery, J. A.; Raghavachari, K.; Al-Laham, M. A.; Zakryewski, V. G.; Ortiz, J. V.; Foresman, J. B.; Cioslowski, J.; Stefanov, B. B.; Nanayakkara, A.; Challacombe, M.; Peng, C. Y.; Ayala, P. Y.; Chen, W.; Wong, M. W.; Andres, J. L.; Replogle, E. S.; Gomperts, R.; Martin, R. L.; Fox, D. J.; Binkley, J. S.; Defree D. J.; Baker, J.; Stewart, J. P.; Head-Gordon, M.; Gonzalez, C.; Pople, J. *Gaussian94*; Gaussian Inc.: Pittsburgh, PA, 1995.
(12) Cerius[2], Molecular Simulation Inc., v4.1, Cambridge, UK, 2000.
(13) Ostwald, W. *Z. Phys. Chem.* **1897**, *22*, 289.

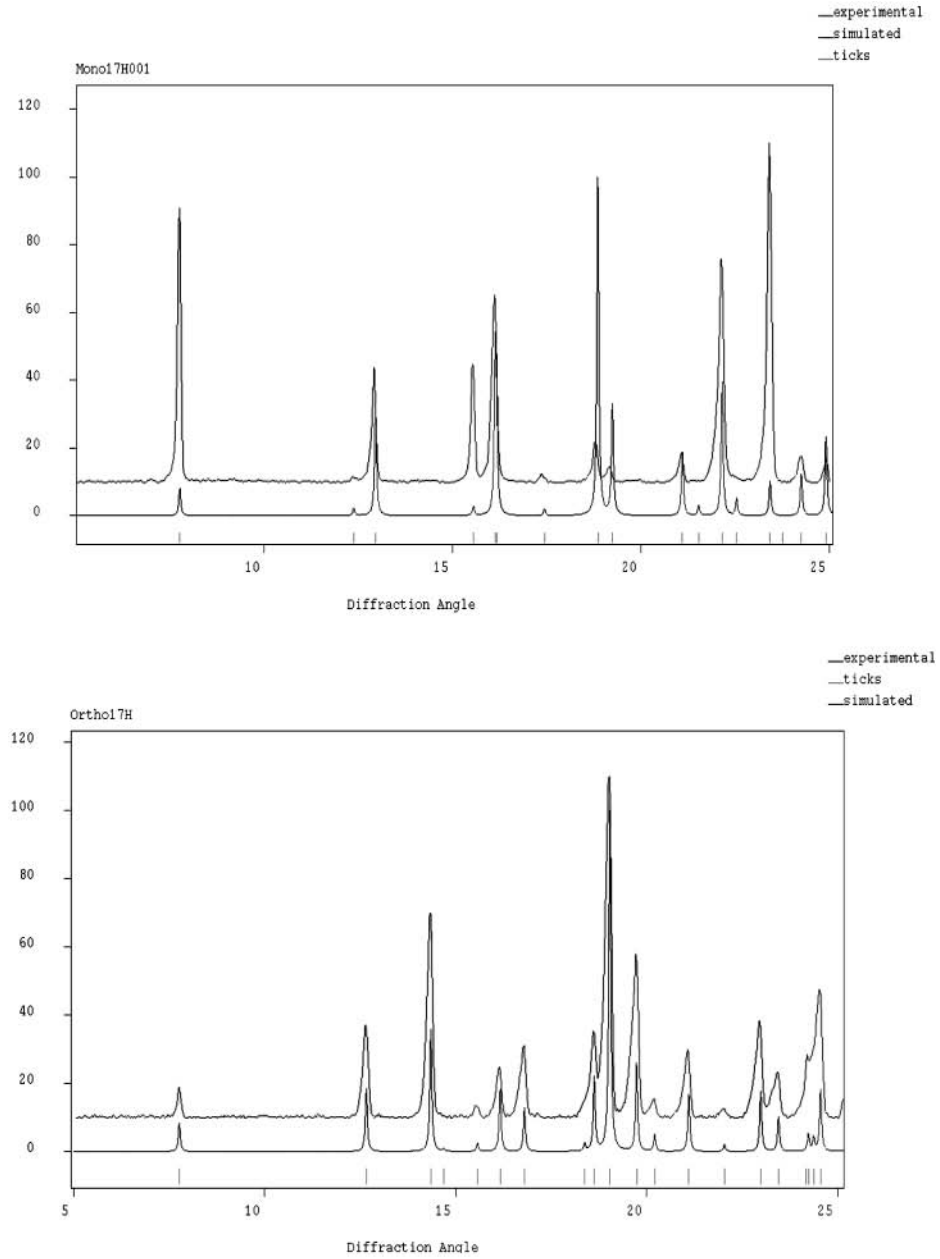

Figure 7. **Calculated and experimental XRPD patterns 17H monoclinic form (top), orthorhombic form (bottom) − diffraction angle 2θ(deg).**

reconstructive mode. Therefore, in consistency with the high melting point of the solute ($T_f \approx 240$ °C), the solid-state polymorphic transition at room temperature is associated with a very poor rate, and our study has been performed in solution. Various parameters were investigated (stirring mode and stirring rate, excess of solid in suspension, seeding or no seeding) using the following experimental setup: 30 mL of saturated solution (plus a mass of solid in excess) of racemic mixture or pure suspension of enantiomer (monoclinic form) were magnetically stirred at 298 K in acetone, ethanol, and 2-methoxyethanol and seeded, or not, with pure crystals of the orthorhombic polymorph (1% w/w). Sampling of the solid phase was periodically performed to monitor the transition by means of XRPD analysis. The polymorphic purity of the solid phase was estimated by superimposition of the experimental XRPD pattern with that calculated from the crystal structures (M and O). The kinetics of transformation were estimated by (i) detecting the orthorhombic form (~5% ortho) or (ii) the complete transformation (100% ortho) of the monoclinic variety. The results are summarized in Tables 7 and 8. Finally, to test the influence of the stirring mode at 2-L scale, a "six-hole square propeller" (7 cm wide) and a "teeth unflocculating" propeller (diameter 5 cm, 12 teethes, with an angle of 100° referred to the rotation axis) were used (solvent acetone, saturated solution at 298 K, solid in excess 4***S***, stirring rate 200 rpm [***S*** is the solubility of the

Table 7. **Rate of the polymorphic transformation in acetone at 298K (*S* = solubility of the racemic mixture); influence of stirring rate and solid in excess**

saturated solution	***S***	***S***	***S***
solid in excess	4***S***	24***S***	4***S***
stirring rate (rpm)	500	500	1000
100% ortho (days)	11	15	8

Table 8. **Influence of seeding on the duration (days) of the polymorphic transformation (monoclinic form to orthorhombic form) at 298 K**

	acetone	acetone	ethanol	ethanol	2 methoxy ethanol	2 methoxy ethanol
racemic[a] mixture	≈ 5%[d] ortho	≈ 100% ortho	≈ 5% ortho	≈ 100% ortho	≈ 5% ortho	≈ 100% ortho
without seed	4	11	8	14	6 weeks	10 weeks
seeded[c]	1	8	1	10	4 weeks	8 weeks
pure enantiomer[b]	≈ 5% ortho	≈ 100% ortho	≈ 5% ortho	≈ 100% ortho	≈ 5% ortho	≈ 100% ortho
without seed	15	18	18	>30	*e*	*e*
seeded[c]	6	9	6	15	*e*	*e*

[a] Saturated solution + 4*S* of solid in excess: monoclinic form only. [b] Saturated solution + 4*S*′ of solid in excess: monoclinic form only. [c] Pure orthorhombic form seeded 1% w/w. [d] 5% ortho = time necessary to obtain 5% of the orthorhombic form in the suspension. [e] Values not determined.

racemic mixture (g/L). Solid in excess 4***S*** means that a mass of solid equal to 4 times the solubility has been added into the suspension.]). Results show that the rate of the polymorphic transformation increases when the shearing effect is enhanced. When the square propeller was used, a complete transformation of $17H_M$ was observed after 10 days; this duration was reduced to 3 days by using the unflocculating propeller.

As expected, the completion of the polymorphic transformation is speeded up with lower excess of solid (2***S*** instead of 4***S***), seeding, high stirring rate, shearing effect, and racemic mixture (the solubility of the racemic mixture is twice that of the enantiomers).

However, whatever the experimental conditions, the rate of the polymorphic transformation, ranging from days to weeks, remains poor.

From the structural and kinetic data depicted above, two opposite effects can be considered: on one hand, structural similarities between the two polymorphic forms ($(100)_M = (200)_O$) could have led to a high heteronucleation rate. On the other hand, the destructive/reconstructive mechanism (combined with a significant value activation energy) and the poor value of $\Delta G = \mu_O - \mu_M$ (lattice energies and solubilities are quite similar for each polymorph) are consistent with slow kinetics.

Indeed, the extensive structural similarities indicate that the crystal slices $(100)_M$ could constitute active sites for the epitaxial nucleation of $(200)_O$ slices.[14,15] A close examination of the particles during the polymorphic transformation showed a significant number of the crystals exhibiting a singular shape (Figure 8), described as a "sandwich" composed of two single crystals exhibiting a plate shape separated by a layer. A possible explanation is that the intermediate layer of the particle is constituted by the monoclinic form upon and below which the orthorhombic phase has nucleated (growth of $(200)_O$ on $(100)_M$ and $(-100)_M$ faces).

Preferential Crystallization (PC). Experimental data presented above have highlighted the slowness of the $17H_M \rightarrow 17H_O$ transition which necessitates days, at least, for completion. As an entrainment is typically a process which lasts 1 or 2 h, the polymorphic transition cannot significantly interfere with the nature of the solid generated by the PC.

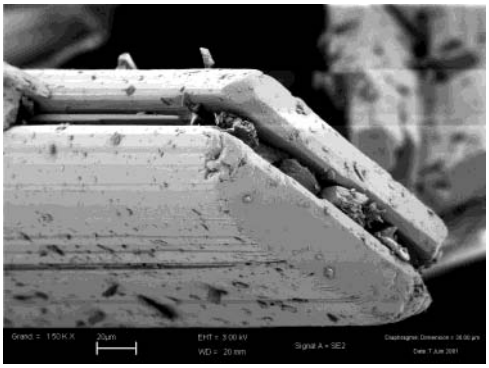

Figure 8. **Aggregate of crystals with a "*Sandwich*" shape observed during the polymorphic transition (monoclinic form to orthorhombic polymorph − 6 mm = 20 μm).**

Table 9. **Initial conditions for PC; evolution of T_{HOMO} in function of the enantiomeric excess; solvent is 2-methoxyethanol**

enantiomeric excess %	0	2	4	6	8
T_{HOMO} (K)	$T_L = 312$	314.2	316.7	319	321.3

Table 10. **Initial conditions for PC: overall enantiomeric excess: 7.4 % (w/w) in 2-methoxyethanol**

mass of solvent (g)	mass of racemic mixture M_R (g)	mass of enantiomer (g)	pure enantiomer (+)-17H seeded (g)[a]	stirring rate (rpm)
1800	368.7	29.7	0.6	250

[a] SIPC only.

Table 11. **Cooling programs**

SIPC	temperature (K)	$333 = T_D$		$287 = T_{Fa}$
AS3PC	temperature (K)	$314.5 = T_B$	285.5	$285.5 = T_{FA}$
	step duration (min)	0	65	95

In view to make valid comparisons between the two processes tested, close experimental conditions have been applied (see Tables 9 and 10). Cooling programs are described in Table 11. Results of PC are summarized in Table 12 and the FBRM curves (population of chord lengths vs time—see Experimental Section) are presented in Figure 9. Figure 10 illustrates the evolution of the rotatory power of the mother liquor during SIPC (a) and AS3PC process (b).

SIPC Process. When the monoclinic form is used as seeds, the in-line monitoring of the chord length population reveals a high secondary nucleation rate almost immediately after

(14) Yu, L. *J. Am. Chem. Soc.* **2003**, *125*, 6380.
(15) Boerrigter, S. X. M.; van den Hoogenhof, C. J. M.; Meekes, H.; Bennema, P.; Vlieg, E. *J. Phys. Chem. B* **2002**, *106*, 4725.

Table 12. **Results of preferential crystallization in 2-methoxyethanol (M = monoclinic, O = orthorhombic polymorph)**

SIPC							
test	seeded form	duration (min)	mass of crude material (g)	optical purity OP (%)	mass of pure enantiomer M (g)	final[a] enantiomeric excess of the mother liquor ee[f]%	polymorphic form of the crops[b]
1	M	23	122	56	68.3	8.48	M
2	M	26	128.3	52	66.7	8.30	M
3	M	24	126.4	55	68.5	8.50	M
4	O	83	94.6	90	85.1	10.35	M
5	O	85	94.8	91	86.2	10.47	M
6	O	83	94.8	90	85.3	10.37	M
15	O	47	94.6	91.3	86.3	10.48	M
AS3PC Auto-Seeding							
test	seeded form	duration (min)	mass of crude material (g)	optical purity OP (%)	mass of pure enantiomer M (g)	final[a] enantiomeric excess of the mother liquor ee[f]%	polymorphic form of the crops[b]
8	M	80	97.1	89	86.5	9.50	M
9	M	77	94.6	92	87	10.55	M
10	M	80	95.2	91	86.6	10.51	M
11	O	93	97.1	89	86.4	10.49	O
12	O	95	94.6	90	85.1	10.35	O
13	O	93	94.6	89	84.7	10.30	O
14	O	333	151	22	33.2	4.31	O
16	O	103	98.2	88.9	87.2	10.58	O

[a] $ee^f\ \% = (M/2) \times 100/[(M/2) + M_R]$. [b] Threshold of detection by means of XRPD ≈ 5%.

the inoculation. The phenomenon lasts ca. 3 min. It results in a large population of small particles (0.8−15.6 μm chords; Figure 9a). The evolution of the rotatory power of the mother liquor (Figure 10a) during the crystallization process (that reflects the counter-enantiomer enrichment in the mother liquor) is similar to the particle size evolution: alpha increases rapidly, showing a strong entrainment effect. Nevertheless, the suspension, composed of fine particles (Figure 11a) is viscous and thus difficult to filter (duration of the filtration is about 10 min, glass filter No. 4). At the threshold of detection by means of XRPD, the crops are only constituted of the monoclinic form.

When the orthorhombic form is used as seeds, the chord length population increases smoothly up to a maximum at 25 min (Figures 9a, 10a). The secondary nucleation rate is poor, and the crystal growth is thus predominant during the whole entrainment process. XRPD analysis of the solid at the end of the entrainment shows that it is solely constituted of the monoclinic polymorph (except the undetected seeds (<2%) of the stable form initially introduced which, therefore have not significantly grown). Due to the large mean crystal size (Figure 11b), the mother liquor is easy to filter (about 1 min). It results in a fairly good optical purity of the crude crops. Because of the good filterability, the overall yield of the process increases (10.4% instead of 8.5% with monoclinic seeds, Table 12).

The polymorphic form of the seeded crystals has a dramatic effect on the course of the entrainment conducted via the SIPC process (i.e. PC initially operated far from equilibrium). When the metastable form is used, an uncontrolled offspring of nuclei is observed; the long duration of the filtration step allows the counter enantiomer to grow in the filtration cake which ultimately reduces the optical purity of the crops and the yield (final enantiomeric excess of the crops, Table 12) of the process. When the orthorhombic form is used as seeds, a damping effect on the initial secondary nucleation is observed. Indeed, as the rate of secondary nucleation of the stable orthorhombic form is quite poor, the high supersaturation at the beginning of the entrainment leads to an epitaxial nucleation and growth of the metastable monoclinic form upon the $(200)_O$ faces of orthorhombic particles. This kinetic process appears to be just the opposite to that observed during the transition M → O depicted in the previous section.[4,14] As the supersaturation decreases during this preliminary step, the secondary nucleation of the monoclinic form takes place in a system which is less far from the equilibrium. Consequently, the stereoselective crystal growth represents an important part of the SIPC process seeded with $17H_O$. The damping effect even at high initial supersaturation acts as if the entrainment was kept under control.

AS3PC Process. By contrast to SIPC process, AS3PC provides a resolution of the racemic mixture, which respects the nature of the initial variety in thermodynamic equilibrium (stable: $17H_O$ or metastable $17H_M$) in the suspension at T_B. At the threshold of detection, the auto-seeded runs with a monoclinic polymorph lead to the enantioselective crystallization of $17H_M$; the pure orthorhombic form is obtained when auto-seeding is performed with $17H_O$. In the former case, (Figure 9b, open symbols), a continuous decrease in small chord length population (0.8−44.3 μm) is observed. Simultaneously, large chord length population (105−149 μm)

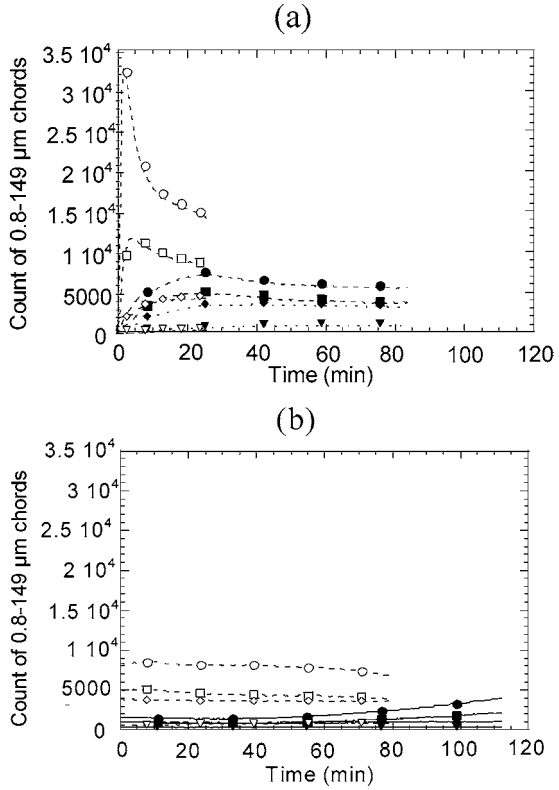

Figure 9. **Evolution of focused beam reflectance measurement (FBRM) curves (chord size distribution (ChSD) of particles) versus time without pretreatment of the solid phase (seeds − SIPC; crystal in equilibrium with the mother liquor at $t = 0$ − AS3PC). (a) SIPC process; open symbols when the racemic mixture is seeded with the monoclinic form; black symbols, the racemic mixture is seeded with the orthorhombic form. (b) AS3PC process; open symbols when the racemic mixture is auto-seeded with the monoclinic form; black symbols, the racemic mixture is auto-seeded with the orthorhombic form. Chord length ranges: ● 0.8−15.6 μm; ■ 15.6−44.3 μm; ◆ 44.3−105 μm; ▼ 105−149 μm. Same scale for number of chords for easy comparison.**

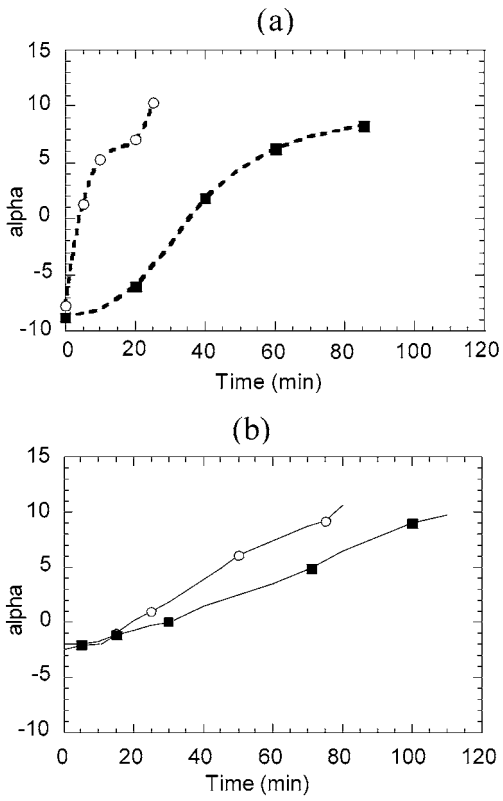

Figure 10. **Evolution of the rotatory power of the mother liquor during SIPC processes (a) and AS3PC processes (b). Monoclinic form seeded (open symbols), orthorhombic form (black symbols).**

slightly increases at the end of the run. When the PC is auto-seeded with the orthorhombic polymorph, a steady state in the chord length distribution is observed for the first 60 min. Subsequently, an increase in the chord length population is noticed except with the 105−149 μm chords length particles which remain constant. Whatever the polymorphic form of the initial particles, these evolutions of the chord length populations versus time (similarly the evolution of the rotatory power of the mother liquor (Figure 10b) illustrate controlled phenomena of nucleation and crystal growth. Crystals isolated at the end of the entrainment always exhibit platelet appearance but size, thickness and specific area differ in accordance with the polymorph used during the self-seeding (Figure 12b). Consequently, the mother liquors are easy to filter: duration of the filtration of about 1 min with $17H_M$, 30 s with the $17H_O$. In both cases, the yield of the process (final enantiomeric excess) reaches 10.5% (Table 12).

In the particular case of run 14 (Table 12), the system has been left on purpose at T_{FA} for 4 h under continuous stirring. XRPD analysis and optical measurement of the filtration cake reveal the presence of $17H_O$ only for both enantiomers. Although some additional hours would have been necessary to attain the thermodynamic equilibrium ($\alpha_{\text{mother liquor}} = 0$), it is clear that a procedure derived from the AS3PC would allow obtaining within some hours 100% of $17H_O$, representing a significant advantage compared to the conversion mechanism $17H_M \rightarrow 17H_O$ depicted in the previous section which necessitates days, weeks, or even months.

Preferential Crystallisation of 17H with Controlled Physical Characteristics of the Initial Particles. Figure 9b shows that in fact the chord length distributions of the two initial populations are quite different (e.g. the number of chord lengths in the 0.8−15.6 μm range is more than 4 times greater for $17H_M$ than for $17H_O$). To avoid any bias in our conclusions, the physical characteristics (crystal size distribution, specific surface area) have been equalized as far as possible.

By means of precipitation in ethanol ($17H_M$) or mechanical grinding ($17H_O$ − Ultra Turrax T25-IKA, 16000 rpm), a racemic mixture and a pure enantiomer of each polymorphic form containing particles of specific area equal to 1.2 m^2/g (a value halfway between results obtained previously) have been prepared. Both SIPC and AS3PC runs were performed at a 35 cm^3 scale using these pretreated solids; the results are summarized in Table 13. When SIPC is applied, the observations reported above without pretreatment are confirmed (nature of solid crystallized: monoclinic form only, very poor filterability when seeding is carried out with $17H_M$, etc.). More quantitatively, $d(\alpha)/dt = 1.67°/\text{min}$ when

Table 13. **Results of preferential crystallization in 2-methoxyethanol using pretreated solids**

					SIPC			
test	seeding form	duration (min)	mass of crude material (g)	OP (%)	mass of pure enantiomer (g)	ee[f]%	polymorphic form of the crops	specific area (m^2/g)
17	M	17	1.53	53	0.81	8.5	M	1.5
18	O	42	1.16	89	1.03	10.8	M	0.8
					AS3PC Auto-Seeding			
test	seeding form	duration (min)	mass of crude material (g)	OP (%)	mass of pure enantiomer (g)	ee[f]%	polymorphic form of the crops	specific area (m^2/g)
19	M	57	1.13	89	1.00	10.5	M	1.4
20	O	63	1.15	95	1.09	11.5	O	0.7

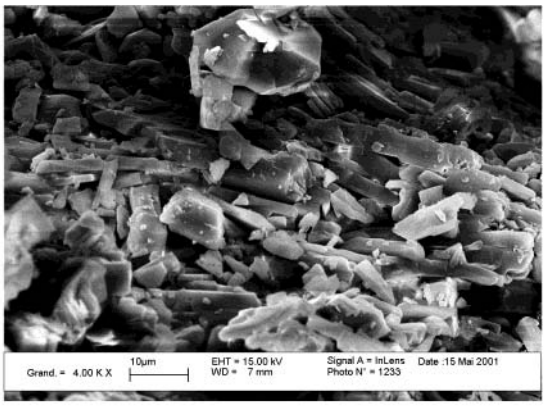

(a – 8mm = 10µm – specific area 2.4m^2/g)

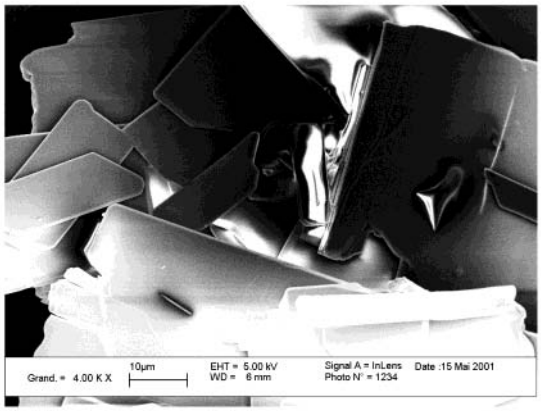

(b - 8mm = 10µm - specific area 0.9 m^2/g)

Figure 11. **SEM photographs of crystals resulting from SIPC process seeded with monoclinic form (a) and seeded with orthorhombic form (b).**

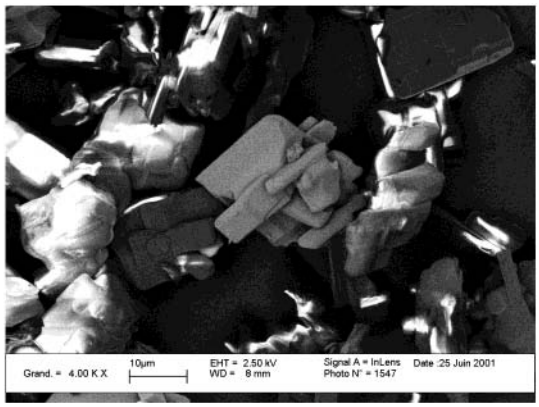

(a – 8 mm = 10µm – specific area 1.6 m^2/g)

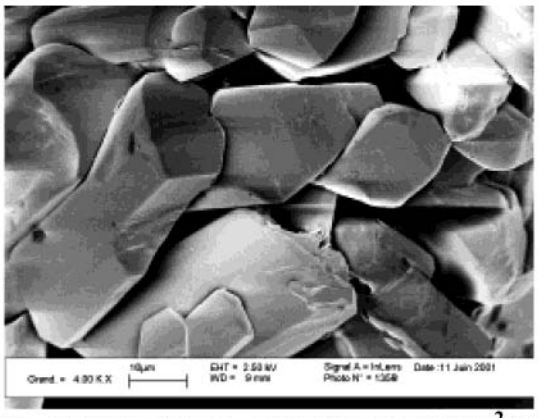

(b - 8 mm = 10µm - specific area 0.7 m^2/g)

Figure 12. **SEM photographs of crystals resulting from AS3PC runs carried out with monoclinic form (a) or with orthorhombic form (b) as initial particles.**

seeded with the monoclinic form, $d(\alpha)/dt = 0.42°$/min when seeded with the orthorhombic form.

When AS3PC process is applied, the intrinsic growth rate of both varieties can be evaluated in the linear part of the cooling program: $d(\alpha)/dt = 0.20°$/min when auto-seeded with the monoclinic form, $d(\alpha)/dt = 0.125°$/min when auto-seeded with the orthorhombic form. The final yield appeared optimum with the following combination: AS3PC process, orthorhombic form submitted to a harsh in situ grinding at T_B.

Conclusions

Despite extensive structural similarities and the possibility of relating the two polymorphic forms by using the DCP model, experimental results indicate that the complete transformation of the $17H_M$ into $17H_O$ is achieved over a long period of time. In accordance with the structural data, this irreversible polymorphic transition proceeds via a destructive/reconstructive mechanism which is solvent mediated. The rate of transformation is mainly limited by the small difference in Gibbs free energies between the initial and the final states which imposes a weak driving force. Without

any particular precaution in the crystallization step, the pure $17H_M$ is always observed, in accordance with the Ostwald law of stages. The nature of the solvent, the mass of solid in excess in the suspension, the inoculation of seeds or not, and various physical factors such as the stirring rate and the stirring mode are determinant parameters to the rate of the polymorphic transition.

Whatever the experimental conditions, the polymorphic transformation is too slow (in the order of days or weeks) to interfere with the durations of the PC (typically 1 or 2 h).

Evidence has been given about the important interrelations between the polymorphic form of the solid at the initial stage of the entrainment and the crystallization process. Invariably, SIPC process leads to the metastable form. When the seeds correspond to the metastable form, a tremendous secondary nucleation is observed just after the inoculation of the solid. It induces the formation of viscous slurry composed of a large population of small particles difficult to filter and thus results in a low optical purity of the crude crops. Any scaling up to large vessels is likely to generate an unmanageable situation.

By contrast, the use of the stable polymorph as seeds induces a smooth offspring of monoclinic crystals by an epitaxial nucleation mechanism which might be the reverse phenomenon to that observed during the lengthy irreversible polymorphic transition. The classical secondary nucleation of the metastable form from the metastable solid occurs afterwards when the supersaturation has decreased, leading to a final population of particles composed of thin platelets—with a good filterability—of the monoclinic variety except for the 1% of the orthorhombic variety added as seeds.

In AS3PC process, the enantiomer in excess is already present as pure particles in the suspension at the very beginning of the cooling (from 25 to almost 50% of the mass of the future crops). The process respects the nature of the initial polymorphic variety: the runs auto-seeded with a monoclinic polymorph lead to the crystallization of the $17H_M$; the orthorhombic form is obtained when using orthorhombic polymorph as initial crystals.

Therefore, with regard to crystallization, the farther the conditions from thermodynamic equilibrium the higher the differences between the behaviours of the two polymorphs. These results are in agreement with the empirical Ostwald law of stages.

As far as the yield of the preferential crystallization is concerned, this study shows that fair comparisons between the four combinations of (i) the variety of the initial solid (monoclinic or orthorhombic form) of the stereoselective crystallization and (ii) the crystallization processes (SIPC or AS3PC), can be considered only when the chord distributions are first equalized by an appropriate pretreatment. The best result is obtained by using the AS3PC process with previously ground orthorhombic crystals. Provided the cooling program will remain slow enough, the scale-up of this procedure will be secure since no perturbing event is likely to appear when using the combination of the stable form of the solid with a smooth and continuously controlled crystallization procedure.

Among the set of chiral molecules crystallizing as stable conglomerates, probably one-third exhibits polymorphism. Therefore, other cases must exist and will be interestingly submitted to investigations. These complementary studies will be of special interest if the polymorphs are related by enantiotropy and if they do not fall into the area of the DCP model treated here (i.e. their structures are completely dissimilar).

Experimental Section

Preferential crystallization was performed in 2-methoxyethanol, at 2-L scale in a thermostated cylindrical reactor, provided with temperature monitoring. The stirring of the medium was kept at 250 rpm throughout the crystallization (stirring propeller). The process was monitored by measuring from time to time the rotatory power (polarimeter Perkin-Elmer 241) of the mother liquor and using the focused beam reflectance measurement technique (FBRM Lasentec). FBRM technique is an in-line method, which allows monitoring the evolution of particles in suspension by measuring their chord lengths during the crystallization. A chord length is two points of the edge of a particle or particle structure (agglomerate). The population of 3D particles is thus represented in a 1D space by means of the chord length distribution. FBRM allows the monitoring of thousands of chords per second, producing a chord length distribution over the range 0.8−1000 μm. At the end of the run the crude crops obtained were filtered off on a glass filter (glass filter No. 4, diameter 10 cm), and the filtration cake obtained (crude material) was dried at room temperature. The specific surface of solids was measured by recording N_2 adsorption isotherms and using Brunauer, Emett, and Teller (BET) method for calculation (Coulter SA 3100 Analyser). Crystal morphologies were observed by means of an electron microscope (SEM LEO with FEG Shottk).

Acknowledgment

This work has been partially supported by INTERREG IIIA network (EU FEDER).

Received for review May 15, 2003.

OP030022G